

A Comprehensive Real-World Evaluation of 5G Improvements over 4G in Low- and Mid-Bands

Muhammad Iqbal Rochman*, Wei Ye[†], Zhi-Li Zhang[†], and Monisha Ghosh*

*University of Notre Dame, [†]University of Minnesota Twin Cities.

Email: *{mrochman,mghosh}@nd.edu, [†]ye000094@umn.edu, [†]zhzhang@cs.umn.edu

Abstract—With the proliferation of 5G and developments of 6G technologies already underway, understanding the real-world performance of various 5G enhancements such as higher modulation, beamforming, and MIMO of deployed 5G over 4G is vital. This work addresses this knowledge gap by conducting extensive 4G/5G measurements in low- (<1 GHz) and mid-bands (1 to 6 GHz) across Chicago and Minneapolis. As both 4G and 5G utilize low- and mid-band channels, we carefully analyze their performance and signal parameters to reveal several key observations: (i) 5G’s throughput improvement today is mainly driven by wider channel bandwidth in the mid-bands, from both single channels and channel aggregation, (ii) realizing further throughput gains necessitates better signal conditions achievable through denser deployment and/or beamforming, (iii) channel rank analysis shows real-world channel conditions rarely support the full 4x4 MIMO, (iv) advanced features like MU-MIMO and higher order modulation like 1024-QAM have yet to be widely deployed, and (v) aggregated throughput performance in LTE can be enhanced by incorporating shared and unlicensed bands, resulting in a performance similar to single-channel NR. These observations and conclusions suggest that the next generation of cellular systems should prioritize wider channels, possibly with enhanced channel aggregation, and a denser deployment architecture utilizing more beams. This would ensure consistently better signal strength across the coverage area with up to 4 MIMO layers per user.

Index Terms—5G, 4G, mid-band, low-band, measurements.

I. INTRODUCTION

5G New Radio (NR) networks have become essential for the advancement of next-generation mobile applications, including augmented and virtual reality, remote vehicle operation, and cloud-based gaming. Recent measurements from the studies [1] indicate that current commercial 5G networks, when operating under optimal coverage conditions, can achieve average downlink speeds of 700 Mbps, with peak performance approaching 1 Gbps, even in urban driving scenarios. This performance represents a substantial leap over 4G LTE networks. The enhancement is largely due to the deployment of cutting-edge wireless technologies such as massive MIMO [2], beamforming [3], advanced modulation techniques [4], and broader bandwidth allocation. The mid-band spectrum, ranging from 1 to 6 GHz, plays a critical role in the success of 5G, offering a balanced trade-off between coverage and capacity [5]. Nonetheless, certain advanced 5G technologies

TABLE I: Statistics of 4G/5G dataset.

Mobile Operators	AT&T, T-Mobile, Verizon
Radio Technologies	4G, 5G
Measurement Venues	Minneapolis, Chicago
Cumulative Data Traces	1200+km; Around 14 hours
XCAL Key Perf. Indicators	PCI-Beam idx; Freq.; SCS; RSRP; RSRQ; CQI; RI; BLER; MCS; #RBs; #MIMO layers; MIMO modes; PHY-layer throughput;

are still in the development pipeline or may be excluded from deployment due to cost issues. Furthermore, because the commercial rollout of 5G has been gradual, earlier studies lack insights into the most recent deployments, particularly in the BRS (2.5–2.7 GHz) and C-band (3.7–4.2 GHz) frequencies. Evaluating how efficiently 5G uses the spectrum is crucial for deciding whether additional spectrum should be allocated for mobile broadband services.

In this paper, we concentrate on the physical layer of 4G and 5G networks, analyzing the characteristics of deployed radio channels and their influence on throughput performance, with a particular focus on low-band and mid-band frequencies, especially the recent NR deployments in the BRS [6] and C-band [7, 8]. Our study aims to answer key questions: What are the similarities and differences in the channel resources and radio technologies currently utilized in 4G and 5G networks? Crucially, is the enhanced performance observed in 5G primarily due to increased bandwidth, or do other innovative technologies significantly contribute? Furthermore, can we quantify the relationship between these factors and their impact on throughput? We believe that addressing these questions could lead to a reassessment of mobile network evolution and provide valuable insights for the design and deployment of future 6G networks.

To accomplish our goals, we undertook comprehensive field measurements in two key metropolitan areas in the US—Minneapolis and Chicago—along with the connecting highways, as depicted in Fig. 1. For data collection, we relied on commercial smartphones as user equipment (UE) and employed a specialized network analyzer to capture and log all network events and key performance indicators (KPIs). The data we collected covers a driving distance of over 1200 km, traversing both 4G and 5G networks of the three major US operators—AT&T (ATT), T-Mobile (TMO), and Verizon (VZW)—as detailed in Table I (see §III for details). To the best of our knowledge, this study is among the first to conduct an extensive, city-wide analysis across two major cities, specifically targeting the improvements that 5G brings over 4G, with an emphasis on the low- and mid-band frequencies.

This research is supported in part by the National Science Foundation under grant numbers CNS-2128489, 2132700, 2220286, 2220292, 2226437, and 2229387.

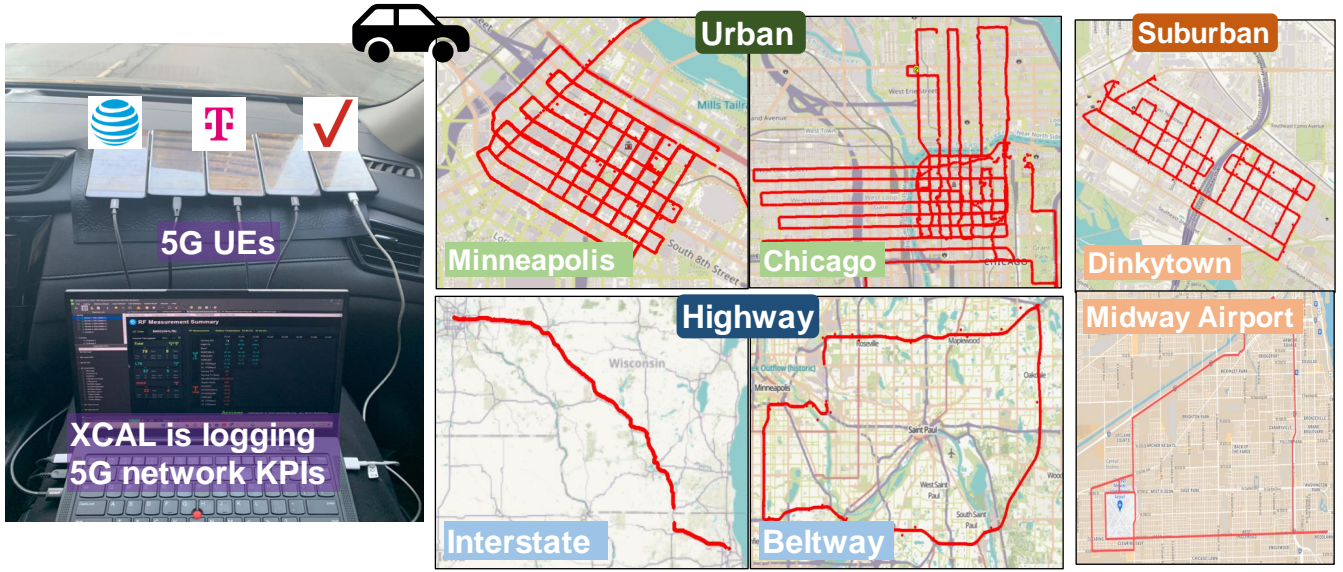


Fig. 1: Setup of the 5G probes and driving routes of our measurements.

Using these datasets, we perform comprehensive data analysis and present our key findings as follows:

(1) Downlink Throughput Comparison Between NR and LTE (§IV-C): We conducted a comparative analysis of downlink throughput across representative low- and mid-band channels in both NR and LTE. As anticipated, NR mid-band channels outperform other NR and LTE channels in both downlink and uplink scenarios. However, after normalizing the throughput, our analysis reveals that the increased channel bandwidth in mid-band 5G is the primary driver behind the enhanced throughput, rather than the introduction of new 5G-specific features.

(2) Influence of Deployment Density and Beamforming on Downlink Throughput (§IV-B): We examined the base station (BS) deployment density and beamforming strategies employed by the three carriers. Our findings indicate that denser deployments, coupled with the use of multiple beamforming modes in the mid-band, significantly enhance overall signal strength, leading to improved spectral efficiency and, consequently, better downlink throughput.

(3) Contribution of Signal Parameters to Normalized Downlink Throughput (§IV-C2, §IV-C3): We analyze how various signal parameters—such as Reference Signal Received Power (RSRP), Modulation Coding Scheme (MCS), Channel Quality Indicator (CQI), and Block Error Rate (BLER)—affect normalized downlink throughput. Our analysis shows that these parameters in NR yield performance comparable to their LTE equivalents. Additionally, we observe the absence of 1024-QAM modulation, which was introduced in the latest 3GPP Release 17.

(4) Comparison of Downlink Throughput in NR and LTE with Channel/Carrier Aggregation (CA) (§IV-B2, §IV-C4): As LTE and NR channels perform in aggregation, we also investigate their CA performance. We observe that dense deployment and availability of secondary channels contribute to higher aggregated DL throughput in NR. Meanwhile, incorporating shared and unlicensed bands increases number of

aggregated channels, thus increases total aggregated bandwidth and enhances throughput performance in LTE CA.

(5) Analysis of Uplink Throughput and Signal Parameters between NR and LTE (§IV-D): Our analysis of uplink throughput reveals that mid-bands generally achieve higher throughput due to their increased bandwidth. There is a direct correlation between MCS and normalized uplink throughput of LTE and NR channels, possibly due to predominant use of 1 layer. Additionally, the newly introduced Pi/2-BPSK modulation, intended to enhance power efficiency in uplink transmissions for 5G, sees limited utilization: its impact on overall performance remains to be fully observed. Interestingly, we observe no instances of uplink CA in LTE nor in NR.

(6) Evaluation of MIMO Performance in NR vs. LTE (§IV-E): Our comparative analysis of the Rank Indicator (RI) reveals a slight improvement in MIMO performance with NR compared to LTE, particularly in terms of the supported channel rank and the number of layers the physical channel can accommodate. Additionally, we observed that Multi-User MIMO (MU-MIMO) has not yet been implemented in the cities included in our study.

(7) Latency Performance Comparison Among NR-SA, NR-NSA, and LTE for T-Mobile (§IV-C, §IV-F): Given that T-Mobile is the sole operator with extensive NR-SA deployment, we evaluated the latency performance of NR-SA, NR-NSA, and LTE networks. Our analysis shows that mid-band NR-SA offers superior latency performance, attributed to its reduced signaling overhead compared to NR-NSA and the benefits of denser mid-band deployments.

II. BACKGROUND AND RELATED WORK

The 5G standard leverages several emerging technologies to enhance network efficiency, most notably high-order quadrature amplitude modulation (QAM), massive MIMO, and beamforming. High-order QAM increases the amount of data transmitted per symbol interval, with 1024-QAM being

introduced in 5G Release 17 [4]. Beamforming concentrates signal energy toward specific users, significantly enhancing both coverage and capacity [3, 9], and is particularly vital for mmWave frequency operations. Prior research [10] has explored the deployment of mmWave 5G in Chicago, identifying how the number of beam indices correlates with beam width and affects handover efficiency. Beamforming is also utilized in lower frequency bands, with each beam linked to a distinct Synchronization Signal Block (SSB) index. Up to eight beams can be utilized by TDD channels operating between 1.88 GHz and 6 GHz using 30 kHz subcarrier spacing, which includes the mid-band BRS and C-band discussed in this work [11]. With beamforming, Massive MIMO or Multi-User MIMO (MU-MIMO) enables superior spatial multiplexing, allowing multiple users to be served simultaneously. However, it faces challenges such as "pilot contamination" [2, 12, 13]. To address this, 5G utilizes channel state information reference signals (CSI-RS) for downlink channel estimation and sounding reference signals (SRS) for uplink estimation [4, 14].

While 4G mobile networks primarily operated on the low (<1 GHz) and mid (1–6 GHz) frequency bands—collectively known as frequency range 1 (FR1) [15]—early 5G deployments in the US have largely focused on the mmWave bands (>24 GHz), referred to as frequency range 2 (FR2). Despite mmWave bands delivering throughput surpassing 1 Gbps, their performance is limited by challenges such as propagation loss, body obstruction, foliage interference, and thermal effects, as shown in our previous research [10, 16]. In contrast, while low-band frequencies offer excellent coverage, they sacrifice bandwidth, which in turn limits throughput. As a result, the mid-band spectrum, which strikes an optimal balance between coverage and performance, has become the cornerstone of current 5G deployments. For example, T-Mobile is advancing its use of the BRS band [6], while AT&T and Verizon are concentrating their efforts on the C-band [7, 8]. Additionally, Verizon is leveraging the CBRS band (3.55–3.7 GHz) within its 4G network, utilizing both Tier 2 PAL and Tier 3 GAA modes [17]. Meanwhile, AT&T and Verizon have also extended their 4G networks into the unlicensed 5 GHz spectrum through License Assisted Access (LAA) [18].

III. MEASUREMENT SETTINGS AND METHODOLOGY

Three measurement campaigns were conducted to collect the data analyzed in this paper. The first campaign took place in Chicago in December 2022. Subsequently, two campaigns were conducted in Minneapolis: one from April to May 2023 and another in November 2023. Both Minneapolis campaigns focused on evaluating the downlink and uplink throughput performance of the three major US operators (ATT, TMO, and VZW). In addition, a dedicated campaign targeting the latency of the T-Mobile network was conducted in Minneapolis in March 2024. Data collection was performed while driving to achieve wider coverage. Fig. 1 displays the 5G probe setup and the driving routes: measurements in Chicago encompassed the downtown Loop area, Midway airport, and the interstate highway; while in Minneapolis, the survey covered Downtown, Dinkytown, and the beltway. Table I provides a summary of the collected data statistics.

We captured all data using Samsung Galaxy S22+ (Android 12) phones, the only devices at the time capable of capturing T-Mobile's inter-band 5G CA. These state-of-the-art phones, which can receive 5G signals in the low-band, mid-band, and mmWave channels, allowed us to measure the network's best possible performance. Three S22+ phones served as user equipment (UE), each equipped with ATT, TMO, and VZW SIMs, all with unlimited data plans and no throttling of data rates. The S22+ phones were connected to a Lenovo ThinkPad X1 Carbon laptop running Accuver XCAL [19]. XCAL establishes a low-level interface to the modem chipset, collecting various 4G and 5G signal parameters. It processes data over one-second periods to account for differences in parameter sampling intervals, averaging numerical values and determining the mode for discrete values. Table II summarizes the key performance indicators collected by XCAL for our analysis, and a glossary of 3GPP terms with references to 3GPP documents [4, 11, 15, 20–25]. XCAL also actively generates full-buffer downlink and uplink traffic using the iperf [26] tool to cloud servers in either Chicago or Minneapolis, depending on proximity to the measurement location.

IV. MEASUREMENT RESULTS AND ANALYSES

A. Overview of the Observed 4G and 5G Deployments

Table III compares the 4G and 5G features we observed to the 3GPP specifications in Release 16 and 17. We believe that most deployments today are at most Release 16. Up to 256-QAM is observed in both LTE and NR networks, but not 1024-QAM. We also did not observe improvements in the number of MIMO layers/streams for low- and mid-band 5G over the 4G counterparts, even though 3GPP Rel-16 supports up to 8 layers. On the other hand, there are improvements in maximum channel bandwidth, as new spectrum has been released. This is reflected in the reduced number of aggregated channels: as bandwidth increases, there is less need to increase CA in 5G.

NR has two modes of network deployments: SA which only utilizes the 5G channels and network stack, and NSA which utilizes a combination of 4G and 5G channels and stacks with 4G used as the primary carrier. Fig. 2 illustrates the operator deployments in downtown and suburban Minneapolis. We observed widespread deployment of NR in NSA mode for ATT and VZW, while TMO densely deployed NR in SA mode. This observation also holds true for the measurement locations in Chicago. In addition to 5G SA and NSA deployments, operators have also deployed Dynamic Spectrum Sharing (DSS), a technology that allows 4G LTE and 5G NR to coexist in the same frequency band by dynamically allocating 4G and 5G resources on a subframe-by-subframe basis. [27]. We observed Verizon's initial DSS deployment around 2019 during the early stages of 5G roll-out when C-band is not available. However, our latest data did not show explicit indications of its usage. While it is possible that Verizon's network still utilizes DSS in some capacity, our UEs, which primarily connect in 5G SA or NSA modes, may not provide visibility into such deployments.

Table IV shows the summary of captured NR and LTE bands/channels in the campaign. NR channels have the prefix "n" and LTE channels have the prefix "b" in the table.

TABLE II: Key performance indicators (KPIs) captured by XCAL.

KPI	Description	3GPP Reference
PCI	Physical cell ID [int]	TS 38.211
SSB beam index	Synchronization Signal Block beam index [int]	TS 38.213
Channel/cell type	Channel/cell types, <i>i.e.</i> , primary or secondary.	TS 38.300
Band	Index of a range of radio frequencies allocated for a specific purpose [int]	TS 38.101
Frequency	Center frequency of a band [MHz]	TS 38.101
Bandwidth	Range of frequencies available for transmission [MHz]	TS 38.104
Duplex Mode	Method of separating uplink and downlink transmissions [TDD/FDD]	TS 38.211
RSRP	Reference signal received power [dBm]	TS 38.215
RSRQ	Reference signal received quality [dB]	TS 38.215
SINR	Signal to interference and noise ratio [dB]	TS 38.214
CQI	Channel quality indicator [int]	TS 38.214
BLER	Block level error rate [%]	TS 38.214
MCS	Modulation and coding schema [int]	TS 38.214
Modulation Mode	Modulation system that describes the number of distinct symbols that can be transmitted per carrier signal, <i>e.g.</i> , QPSK, 16-QAM, 64-QAM, 256-QAM.	TS 38.211
#Layers	Number of MIMO layers [int]	TS 38.214
RI	MIMO rank index [int]	TS 38.214
PMI	Precoding matrix index [int]	TS 38.214
#RBs	Number of allocated resource blocks [int]	TS 38.211
Tput	Physical layer throughput in downlink and uplink directions [Mbps]	TS 38.306
RRC messages	Radio resource control messages, such as measurement report triggering, connection status, etc.	TS 38.331

TABLE III: Highlight of features in 3GPP Rel-16 and Rel-17 compared to observed 4G and 5G in our dataset.

Parameters	Observed 4G	Observed 5G	Rel-16 5G	Rel-17 5G
Max. Modulation	256-QAM	256-QAM	256-QAM	1024-QAM
Max. MIMO Layer	4	4	8	8
Max. Ch. BW (excl. mmWave)	20 MHz	100 MHz	100* MHz	100* MHz
Max. #CA	6	4	16	16

*mmWave channels can be up to 400 MHz wide

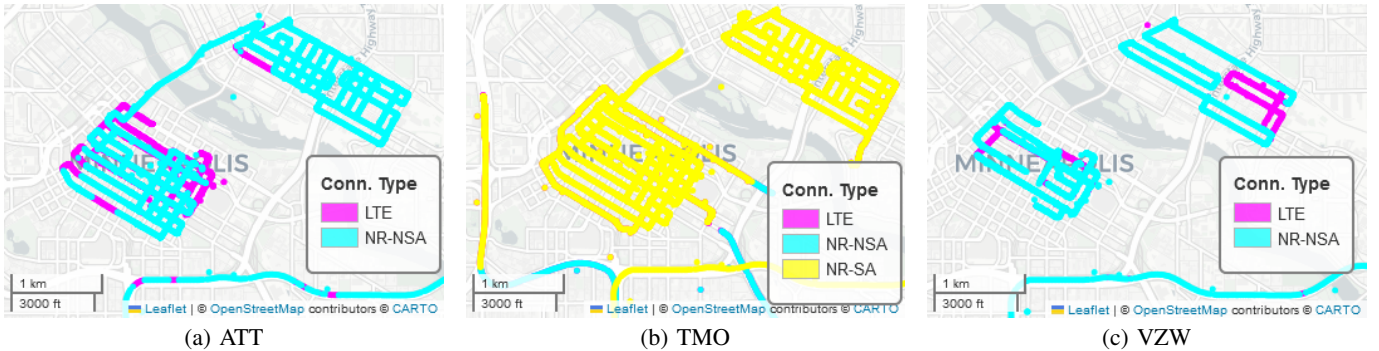


Fig. 2: Map of signal reception by the connection type at the downtown and suburban Minneapolis.

All three operators have deployed NR in low- and mid-bands. Notably, ATT-n66 and TMO-n25 are the newest bands detected only in our April-May 2023 campaign and afterward. AT&T and Verizon have also deployed NR mmWave bands (n260 and n261), but they are out of scope for this analysis. Among the NR low- and mid-band channels, all FDD channels are deployed with 15 kHz sub-carrier spacing (SCS) and lower bandwidth (*i.e.*, ATT-n5, ATT-n66, TMO-n25, TMO-n71, VZW-n5), while all TDD bands are deployed with 30 kHz SCS and higher bandwidth (*i.e.*, ATT-n77, TMO-n41, VZW-n77). These deployments suggest that the NR FDD bands are positioned as the “support” bands since the lower bandwidth and frequency result in lower throughput but greater coverage. It should be noted that TMO’s mid-band deployment in 2.5 GHz has a 3.4 dB advantage over ATT and VZW in 3.7 GHz: this will be seen in performance results presented later. Most of the deployed LTE channels are FDD, except for the newer b46 (LAA) and b48 (CBRS) which are TDD, and b29 which is a supplementary downlink (SDL) band. The LTE bands are similarly used as the “support” bands to the NR TDD bands

when aggregated in the NSA deployments.

While we observed low- and mid-band 5G deployments from the operators, our findings also highlight the need for them to further develop their 5G networks to meet the full capabilities outlined in 3GPP Release 16 and 17. Operators should prioritize acquiring new spectrum and transitioning to 5G Standalone (SA) mode to enable full utilization of advanced 5G features.

B. Comparison of Low- and Mid-band Deployment

In this section, we compare low- and mid-band channels in terms of coverage density and available bandwidth. These are significant factors that gives context to our throughput analysis in the next section. Preliminary analysis revealed negligible differences between the datasets collected in Chicago and Minneapolis. Consequently, we combined them for the analyses presented in this paper. For brevity, we selected a representative low-band and mid-band channel for each operator with substantial data points, regardless of their primary

TABLE IV: NR and LTE Bands Information

Operator-Band	Duplex Mode	DL Band Freq. (MHz)	SCS (kHz)	BW (MHz)
Representative Bands				
ATT-n5	FDD	850	15	10
ATT-n77	TDD	3700	30	40
TMO-n41	TDD	2500	30	40,100
TMO-n71	FDD	600	15	20
VZW-n5	FDD	850	15	10
VZW-n77	TDD	3700	30	60
ATT-b2	FDD	1900	15	20
ATT-b12	FDD	700	15	10
ATT-b46	TDD	5200	15	20
TMO-b12	FDD	700	15	5
TMO-b41	FDD	2500	15	20
TMO-b66	FDD	2100	15	20
VZW-b13	FDD	700	15	10
VZW-b48	TDD	3500	15	10,20
VZW-b66	FDD	2100	15	20
Other Bands				
ATT-n66	FDD	2100	15	5
TMO-n25	FDD	1900	15	20
ATT-b14	FDD	700	15	10
ATT-b29	SDL	700	15	5
ATT-b30	FDD	2300	15	5,10
ATT-b66	FDD	2100	15	5,10,15
TMO-b2	FDD	1900	15	10
TMO-b4	FDD	2100	15	20
TMO-b25	FDD	1900	15	10
TMO-b46	TDD	5200	15	20
TMO-b71	FDD	600	15	5
VZW-b2	FDD	1900	15	10
VZW-b4	FDD	2100	15	20
VZW-b5	FDD	850	15	10
VZW-b46	TDD	5200	15	20

or secondary cell/channel designation. All mid-band channels are deployed with higher bandwidth compared to low-band channels.

1) *Comparison of 4G and 5G coverage density:* Table V summarizes our analysis of low- and mid-band deployment density, based on data points, unique Physical Cell Identifiers (PCIs), and the number of SSB beams for selected channels. Recognizing that PCI assignment practices differ (single per base station or multiple per sector), we do not aim to quantify total deployments. Rather, we examine the interplay between unique PCIs and the number of SSB beams, as a high number of both indicates a denser deployment with finer beam steering and potentially higher beamforming gain. Due to PCI reuse, the number of unique PCIs is calculated separately between Chicago and Minneapolis.

Number of data points and unique PCIs: For ATT NR, n77 (mid-band) and n5 (low-band) are selected due to the higher amount of captured data. Further, n5 has a larger number of data points and unique PCIs, indicating a denser deployment in the low-band: this is in contrast to TMO and VZW which have a higher number of data points and unique PCIs in mid-bands (TMO-n41 and VZW-n77, respectively) compared to low-bands (TMO-n71 and ATT-n5, respectively). Moreover, TMO-n41 is very densely deployed with 462 unique PCIs compared to the NR channels from ATT and VZW. As we shall see later, the density of the TMO NR deployment and the lower NR mid-band frequency (2.5 GHz) significantly impact overall superior signal strength, spectral efficiency, and throughput compared to ATT and VZW.

Similar to the NR bands, we observe a higher number of data points and unique PCIs on mid-band LTE channels compared to low-band. For ATT, b66 has the largest number

TABLE V: Rep. Bands' Deployment

(Bands in bold are mid-bands.)

Operator-Band	n data	% data	#SSB Inds.	#unique PCI
ATT-n77	8380	34	1,6*	152
ATT-n5	14444	58	1	217
TMO-n41	56606	90	6	464
TMO-n71	1981	3	1	60
VZW-n77	13049	96	1	147
VZW-n5	541	3	1	28
ATT-b2	31480	28	N/A	378
ATT-b46	7090	6	N/A	77
ATT-b12	12690	11	N/A	262
TMO-b66	19334	39	N/A	330
TMO-b41	7400	15	N/A	54
TMO-b12	2645	5	N/A	83
VZW-b66	31742	36	N/A	379
VZW-b48	8762	8	N/A	141
VZW-b13	16906	19	N/A	255

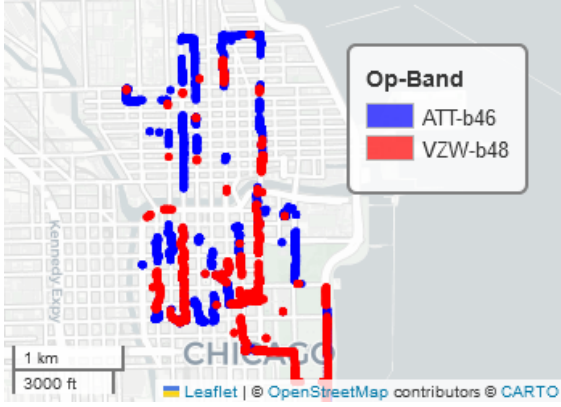
*ATT-n77 has 6 SSB indices in Minneapolis, but only 1 in Chicago.

TABLE VI: DL Channel Combinations.

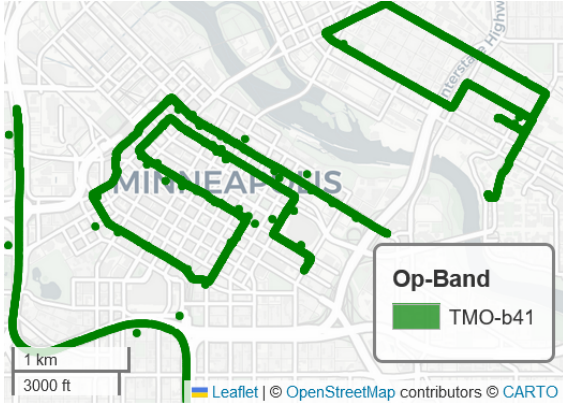
Operator	Channel Combinations	Aggregated BW	Num. Unique
ATT	4G up to 5 channels	Up to 90 MHz	162
	5G n77 + n77	Up to 80 MHz	1
TMO	4G up to 5 channels	Up to 90 MHz	42
	5G n25 + n41 + n41	160 MHz	1
	5G n71 + n25 + n41	135 MHz	1
	5G n41 + n41	up to 140 MHz	3
	5G n25 + n41	120 MHz	1
	5G n71 + n41	up to 120 MHz	7
	5G n25 + n25	25 MHz	1
VZW	4G up to 5 channels	Up to 100 MHz	108
	5G n5 + n77	70 MHz	1

of data points for mid-band. However, we chose the second-largest b2 for its wider bandwidth. For TMO, b12 is the only low-band channel beside b71, indicating the very sparse deployment of low-band LTE in TMO: b12 and b71 channels account for 10% of the total LTE data. The proportion of data and PCIs in mid-band LTE and NR indicates that TMO and VZW have been focusing on mid-band deployments. Lastly, we selected ATT-b46 and VZW-b48 as representatives of the unlicensed/shared mid-band 4G channels. Fig. 3a indicates prominent deployments of ATT-b46 and VZW-b48 only in downtown Chicago. However, these bands exhibited fewer data points and unique PCI compared to other channels, indicating localized deployments with lower power. TMO also deployed b46 channels, but it only accounts for 0.8% of all TMO LTE data, indicating an even limited deployment. Instead, TMO-b41 is chosen for comparison with TMO-n41, with data points observed only at Minneapolis, as shown in Fig. 3b.

Number of beams: Our observations indicate that all operators' 5G networks utilize a form of hybrid beamforming by combining Synchronization Signal Blocks (SSB) and precoding matrix techniques. The precoding matrix, informed by the PMI feedback from the UE, takes advantage of the rich scattering environment to optimize signal transmission, *i.e.*, digital beamforming. On the other hand, SSB-based beam concentrates energy in a particular direction to provide a degree of spatial selectivity, *i.e.*, analog beamforming. In this subsection, we analyze the number of distinct SSB indices used, as this metric reflects the degree of beam refinement employed, which can ultimately lead to improved coverage. Table V shows the number of SSB Indices which denotes the number of beams available for each NR channel. We observe only index 0 (*i.e.*, single beam) per PCI for ATT channels in



(a) ATT-b46 and VZW-b48 in downtown Chicago.



(b) TMO-b41 in Minneapolis.

Fig. 3: Map of signal reception of ATT-b46, VZW-b48, and TMO-b41.

the Chicago campaign. However, we observe 6 SSB indices for ATT-n77 in the later Minneapolis campaign. Fig. 4a shows the coverage of the various SSB Indices for ATT-n77, PCI 290, in Dinkytown. Similarly, Fig. 4b depicts SSB Indices from 0 to 5 for TMO-n41, PCI 58, in downtown Minneapolis. All low-band NR channels, *i.e.*, n5 and n71, only use one SSB index, and the number of SSB indices did not change between the two campaigns. Unlike TMO and ATT, VZW always uses a single SSB index per PCI for all of its NR channels in both cities. Fig. 4c illustrates the coverage of one of VZW’s n77 channels in downtown Minneapolis. Since more SSBs/PCI means more beams and hence beamforming gain, VZW with only one beam/PCI suffers from lower signal strength overall and poorer spectral efficiency, as will be shown later.

2) *Channel combinations*: We also investigate LTE and NR performance in a CA scheme. As our UE captures all LTE and NR channels with its type (*i.e.*, primary or secondary), we can determine the number of channels and the combinations utilized in a CA. Table VI presents the observed channel combinations employed for downlink CA by the three operators, along with their total bandwidth and number of unique CA combinations. Details of LTE CA are omitted due to the extensive number of unique channel combinations. Nevertheless, we observe all operators aggregate up to 5 channels in the LTE. Notable, ATT and TMO achieved 5 CA by aggregating three b46 channels with two licensed channels. Similarly, VZW aggregates their b46 and b48 channels to

achieve 5 CA.

Although 5G CA can significantly boost the aggregated bandwidth up to 800 MHz using mmWave channels, we limit our scope to low- and mid-band CA, where we observe a limited bandwidth due to the limited number of deployed NR channels. There are limited instances of two NR low- or mid-band channels being aggregated in ATT and VZW networks. In contrast, TMO uses diverse channel combinations in both intra-band and inter-band configurations, with up to 3 CCs aggregating to 160 MHz width. For uplink transmission, we did not observe CA in either 4G or 5G. Uplink CA is only possible between one 4G and one 5G channel in the NR-NSA mode.

This subsection has contrasted the deployment strategies of each operator. Although all operators prioritize high-bandwidth mid-band channels, TMO stands out with its denser deployment, evidenced by a greater number of unique PCIs and SSB beams. Moreover, the limited number of available 5G CA combinations when compared to 4G CA, underscores the need for additional spectrum to enhance 5G CA capabilities.

C. Analysis of DL Throughput Performance Between Low- and Mid-Band Channels

1) *Downlink throughput and normalized downlink throughput*: Fig. 5a shows the comparison of downlink (DL) physical layer throughput between low- and mid-band LTE and NR, as reported by XCAL during all of our driving measurements. We observe a considerably higher downlink throughput on the mid-band NR channels compared to the low-band counterparts. As discussed in a prior section, this can be explained by the wider bandwidths. The highest median throughput of 218 Mbps is attained by TMO-n41 with a combination of two NR channels of 40 and 100 MHz bandwidth. For the LTE bands, we similarly observe higher throughputs on mid-band channels compared to the low-bands. The highest median throughput of 39 Mbps is achieved by VZW-b48 with 20 MHz bandwidth. Since all representative channels’ block error rate (BLER) is similar, the increase in median throughput in NR may be attributed to the wider bandwidth.

Thus, we examine channel spectral efficiency for a deeper analysis. This involves normalizing the throughput of each channel by its bandwidth and number of MIMO layers, allowing us to directly compare how effectively each channel utilizes its allocated spectrum. We define normalized throughput: $T_{put_{norm}} = T_{put_{bps}} / (N_{RB} * SCS_{Hz} * 12) / N_{layer}$, where $T_{put_{bps}}$ is the throughput in bits/second, N_{RB} is the average number of resource blocks (RBs) allocated to the UE over one second, SCS_{Hz} is the subcarrier spacing (SCS) in Hz, and N_{layer} is the number of MIMO layers used. To determine the instantaneous bandwidth usage, we multiply N_{RB} by SCS_{Hz} and 12, given that there are 12 subcarriers in each RB. Since we use RB to normalize throughput, the difference between TDD configurations in the mid-band channels should not make a difference. However, we observe that all operators in the mid-band channels use the same TDD configuration of 7 slots for DL and 2 slots for UL (uplink), with a slot length of 0.5 ms. Note that when normalizing LTE throughput, RI is used

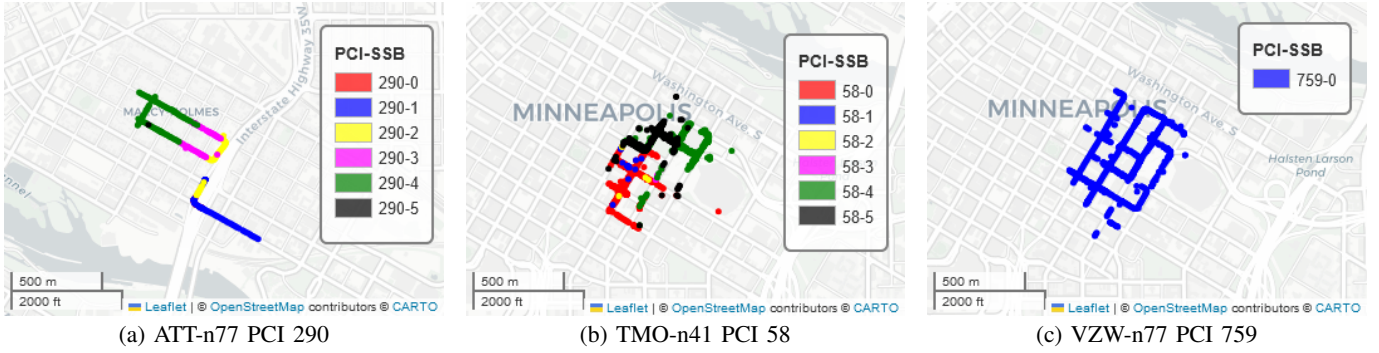


Fig. 4: PCI-SSB index maps of mid-band channels.

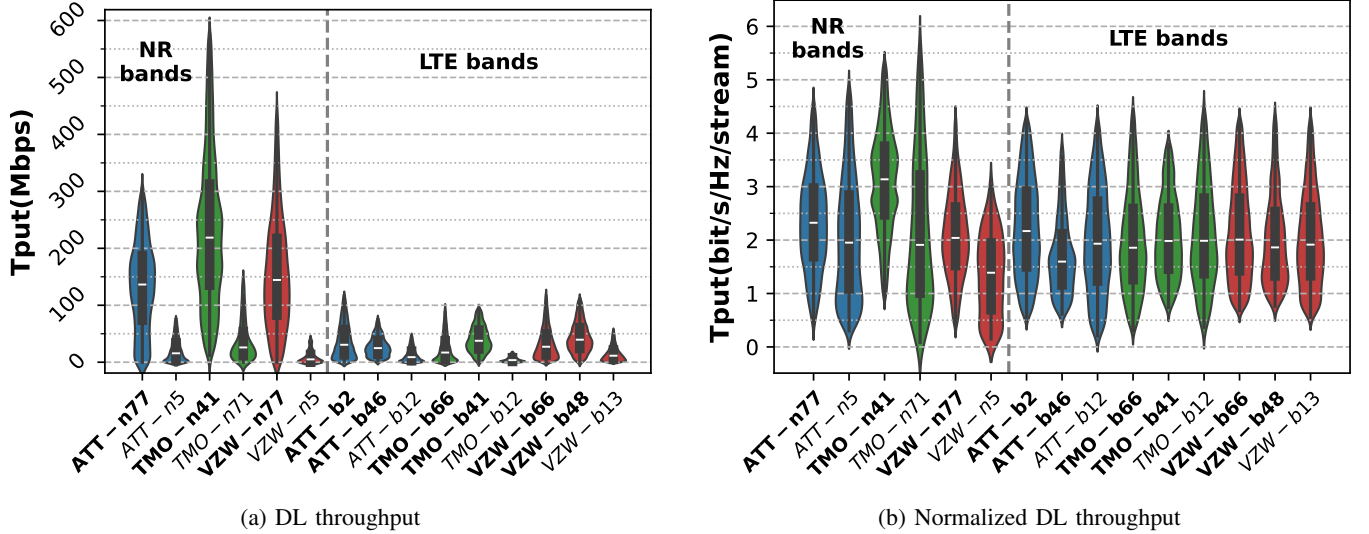


Fig. 5: DL throughput comparison of NR and LTE in low-bands (normal) and mid-bands (bolded)

due to the lack of the MIMO layer number KPI in LTE. This is viable since we observe a Pearson correlation of 0.95 between the RI and MIMO layers in our NR data, which is expected since RI is a part of Channel State Information (CSI) feedback to decide the number of MIMO layers.

As computed above, Fig. 5b compares the normalized throughput (spectral efficiency) of NR and LTE channels. VZW-n5 exhibits the lowest median normalized throughput, while TMO-n41 achieves the highest (3.14 bit/s/Hz/stream). Other channels fall between 1.9 and 2.3 bit/s/Hz, analogous to the theoretical capacity of uncoded QPSK of 2 bit/s/Hz. Since we previously observed a higher throughput from channels with higher bandwidth, this strongly indicates that the increase in throughput from LTE to NR can be attributed primarily to the wider bandwidth and number of MIMO layers. The exception being TMO-n41, which has a much higher spectral efficiency due to its dense deployment (compared to both ATT and VZW) and larger number of beams (compared to VZW), both of which lead to improved overall signal strength and hence spectral efficiency. Furthermore, the stark contrast with TMO-b41, an LTE channel in the same frequency band, confirms that TMO-n41's superior performance stems from its denser deployment. Finally, we find that ATT-b46 exhibits lower normalized throughput compared to VZW-b48. While both channels utilize sharing schemes, ATT-b46's listen-before-talk scheme can introduce contention,

whereas VZW-b48's authoritative access scheme (Spectrum Access System/SAS) grants exclusive access to a specified channel for a 24-hours period. Moreover, b46 channels are limited to a maximum Equivalent Isotropic Radiated Power (EIRP) of 36 dBm over 20 MHz, lower than b48's maximum EIRP of 50 dBm outdoors over 20 MHz (all VZW-b48 deployments are outdoor).

2) *Contribution of RSRP, MCS, CQI, and BLER to normalized DL throughput*: Fig. 6a shows a comparative analysis of the Synchronization Signal RSRP (SS-RSRP) on NR channels, and RSRP on LTE channels. Both ATT and VZW exhibit higher SS-RSRP values on their low-bands in comparison to their mid-band counterparts: this is due to better propagation characteristics of the low-bands. However, mid-band TMO-n41 displays higher SS-RSRP (median of -79 dBm) compared to its low-band counterpart, n71, which indicates a denser NR deployment to overcome the propagation loss at the mid-bands. Furthermore, the distribution of TMO-n41 RSRP is consistently higher compared to other operators' NR mid-bands: ~ 9 dB higher than VZW-n77 and ~ 15 dB higher than ATT-n77. This is due to a combination of dense deployment, multiple beams/PCI, and lower frequency. In LTE, we observe the similarity of RSRP distribution between the channels. The highest median RSRP of -83 dBm is achieved by ATT-b2, which is reflected in the normalized throughput: the highest median downlink throughput of 2.18 bit/s/Hz/stream over all

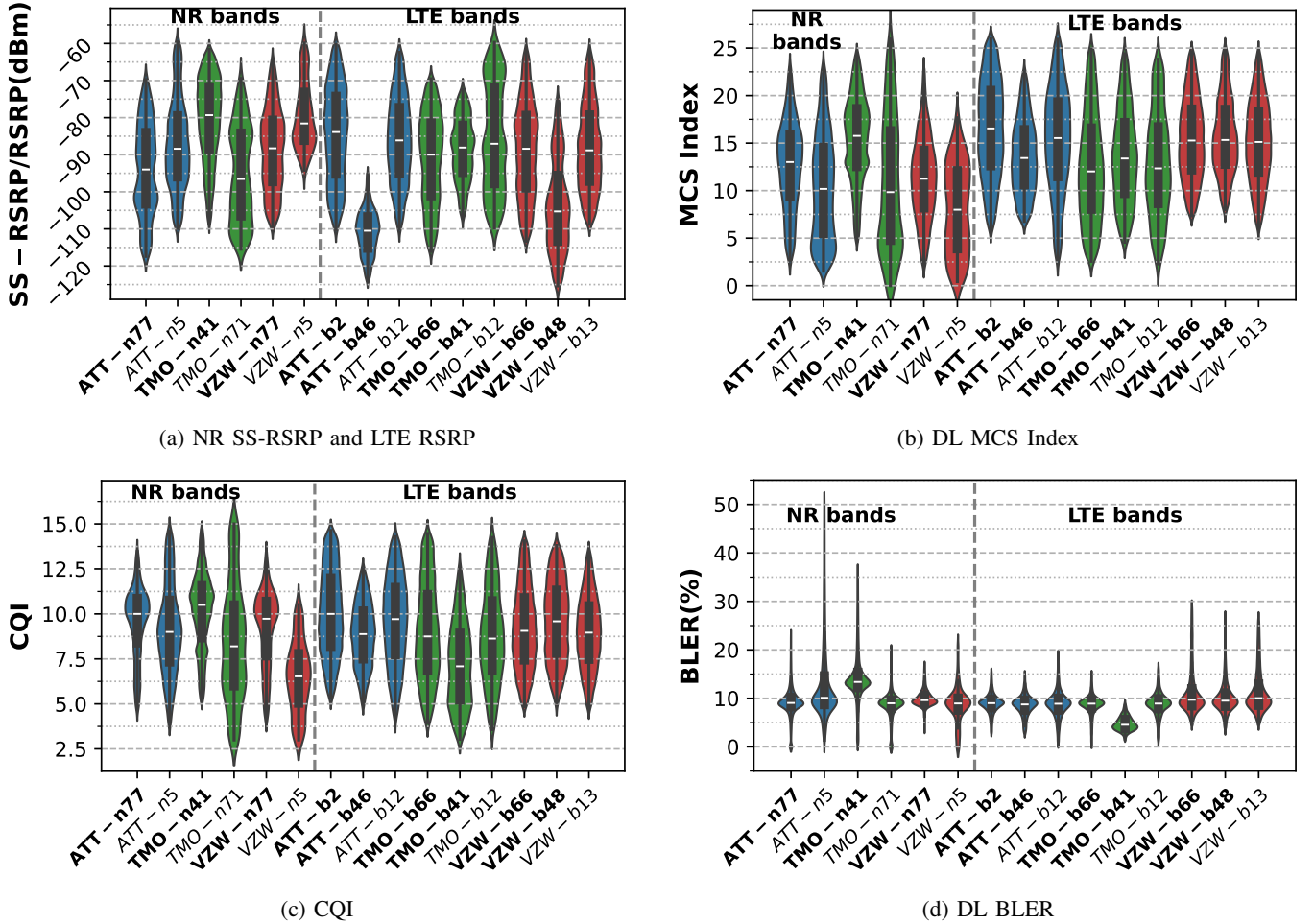


Fig. 6: Comparison of RSRP, DL MCS, CQI, and DL BLER of NR and LTE in low-bands (normal) and mid-bands (bolded).

LTE channels. On the other hand, ATT-b46 and VZW-b48 show lower RSRP due to the limitations of transmit power. Between NR and LTE, TMO-n41 stands out due to its denser deployment and higher number of beams.

Fig. 6b shows the distribution of allocated downlink MCS index, which correlates well with the distribution of normalized downlink throughput in LTE and NR. For instance, the best and worst median MCS index in NR are achieved by TMO-n41 and VZW-n5, respectively, which correspond to the best and worst median normalized downlink throughput. This is expected since higher MCS index delivers higher spectral efficiency but can only be used in good signal conditions. Further, we found RRC messages (“pdsch-Config > mcs-Table := qam256” in NR and “cqi-ReportConfig > altCQI-Table-r12 := all subframes” in LTE) which indicate that both LTE and NR used the MCS Table 2 as described in Table 5.1.3.1-2 of [4], making comparison feasible. We observe a lower median of MCS in NR channels compared to LTE, except for TMO-n41, again due to the excellent channel condition guaranteed by its denser deployment.

We further compare the CQI, which indicates channel conditions from the UE’s perspective. Fig. 6c illustrates the comparison of CQI between the representative LTE and NR channels. Since the BS uses CQI to decide the MCS selection,

the distribution of CQI aligns with its respective MCS values: the highest median CQI is attained by TMO-n41, similar to its median MCS, and vice versa with VZW-n5. On LTE, we also observe a similar distribution of LTE CQI with MCS. This further shows that normalized throughput is mainly influenced by the overall channel condition reported by UE, rather than just RSRP. However, since we cannot ascertain whether the CQI table used by NR and LTE networks are the same, we cannot make a direct comparison between them.

Lastly, we compare BLER as shown in Fig. 6d. For all representative channels, we observe a distribution with high range but low variance which indicates a strict error target: a characteristic feature of CQI. All representative channels show median BLER of around 10%, with slight deviations on the highest value achieved by TMO-n41 and the lowest value by TMO-b41. This possibly indicates a customized BLER target for said channels.

3) *Comparison of DL modulation modes*: Fig. 7 shows the modulation modes used for the 12 representative low- and mid-band channels as defined in a previous section. Only modulation modes from QPSK to 256-QAM are observed in our campaign. TMO-n41 shows higher usage of 64-QAM and 256-QAM modulation, corresponding to the channel’s high normalized downlink throughput. Conversely, the VZW-

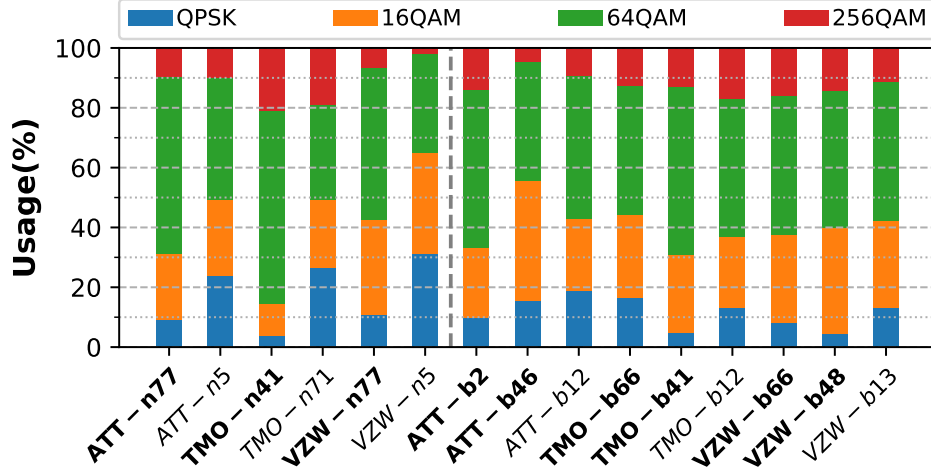


Fig. 7: Proportional usage of DL modulation modes of NR and LTE in low-bands (normal) and mid-bands (bolded).

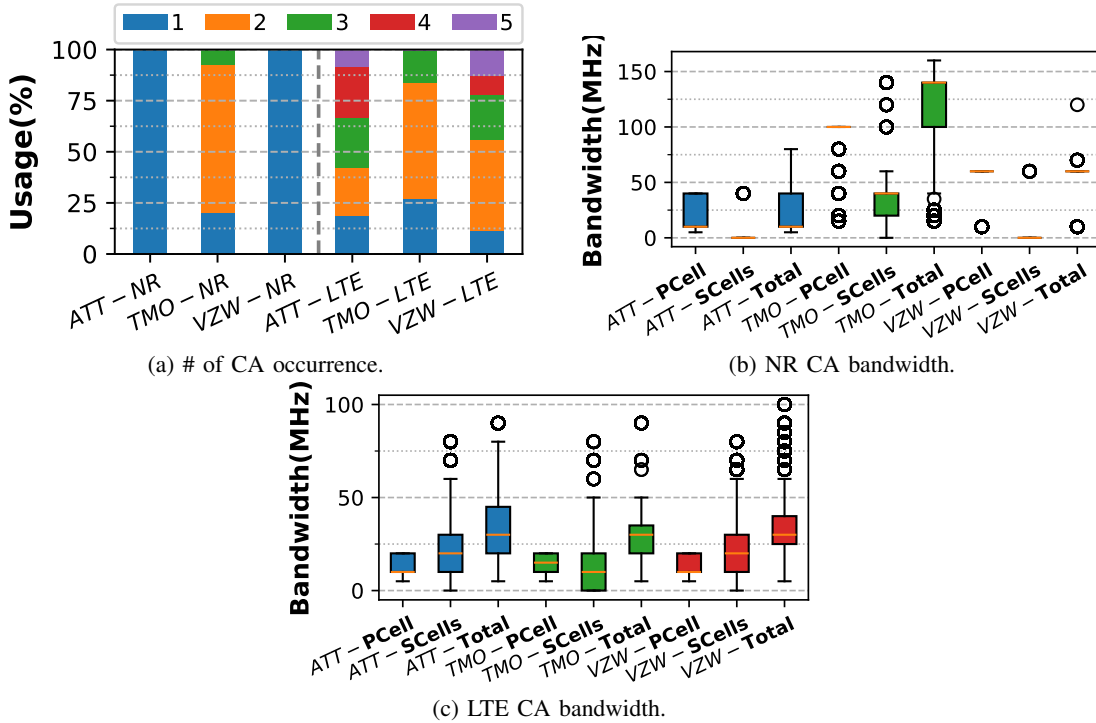


Fig. 8: Number of aggregated DL channels and bandwidth.

n5 channel uses a higher proportion of QPSK and 16-QAM modes, which also explains the low normalized throughput of this channel. For LTE, ATT-b2 mainly uses a combination of 64-QAM and 256-QAM modes, and this results in the highest normalized downlink throughput performance among the LTE channels. Moreover, the resemblance in modulation usage among the other LTE channels corresponds to the similarity in their normalized throughput.

Comparing the modulation modes between the NR and LTE channels, we do not observe a significant improvement, *i.e.*, no indication that higher modulation is more available in NR compared to LTE, except for the TMO NR channels n41 and n71, which use 256-QAM more often than the other carriers. This is due to the fact that TMO exhibits better signal

conditions in general, which confirms that spectral efficiency improvements are only possible if the overall signal strength improves, through a combination of dense deployments and usage of more beams.

4) *Comparison of DL Channel Aggregation Between Operators*: Fig. 8a illustrates the prevalence of CA across all three operators. All operators' LTE networks exhibit extensive CA usage, with up to 5 CA. In NR, we observe up to 3 CA instances in low- and mid-band channels. Fig. 8b details the NR bandwidth distribution among the primary cell/channel (PCell), the combined secondary cells/channels (SCells), and their total. TMO demonstrates a higher total NR CA bandwidth, with a median of 140 MHz achieved using two n41 channels (100 and 40 MHz). While ATT and VZW aggregate up to 2 CA, their median CA count is 1,

resulting in median total bandwidths of 10 and 60 MHz, respectively. As expected, NR SCells bandwidth is lower than PCell due to the limited availability of secondary NR channels. Fig. 8c presents a similar LTE bandwidth breakdown, revealing a median total bandwidth of 30 MHz across all operators. Contrary to NR, LTE SCells bandwidth surpasses PCell, which can be attributed to the higher number of candidate LTE channels that can be assigned as secondary channels.

In Fig. 9a, we present the breakdown of NR throughput in PCell and SCells, as well as the total, on all operators. TMO achieved the highest median NR total throughput of 338 Mbps, with visible contributions from PCell (median 210 Mbps) and SCells (median 113 Mbps). Notably, TMO's PCell throughput is higher compared to other operators, indicating the positive effect of dense deployment with multiple beams that we discussed in prior sections. On the other hand, we observe a median SCells throughput of 0 Mbps for ATT and VZW due to the limited availability of secondary channels in their NR network. To further focus on the impact of SCells, Fig. 9b presents the NR CA throughput breakdown only for CA > 1, where TMO still performs the best in PCell, SCells, and total throughput due to higher bandwidth and secondary channels availability. ATT shows a similar PCell and SCells throughput due to the 40+40 MHz channel combination, while VZW shows lower PCell throughput compared to its SCells due to lower PCell bandwidth of 10 MHz to the SCell bandwidth of 60 MHz. For LTE, Fig. 9c shows a similar breakdown. While CA throughput values in LTE are significantly lower compared to the NR counterparts, we observe higher SCells throughput than PCell due to the greater number of LTE channels available for SCells assignment. Since b46 and b48 channels enable CA ≥ 4 , we focus on Fig. 9d that illustrates LTE CA throughput when b46 or b48 channels are included. Here, SCells and total throughput are considerably higher for all operators compared to Fig. 9c, even approaching ATT & VZW NR levels. This underscores the importance of a higher number of CA enabled by the b46 and b48 channels.

In this subsection, we observed high downlink throughput achieved by high-bandwidth mid-band channels. While operators typically focus on deploying wider bandwidths and more channels to boost throughput, our analysis clearly demonstrates the critical role of increased coverage density. Higher density not only improves channel quality but also enables the higher-order modulation schemes that are key to 5G's performance advantages. Furthermore, our 4G CA analysis suggests that shared channels, such as b46 and b48, could serve as a temporary solution for enhancing downlink throughput.

D. Analysis of Uplink Throughput Performance Between Low- and Mid-Band Channels

Fig. 10a illustrates that overall UL throughputs are lower than their downlink counterparts across all representative bands due to the fewer streams utilized. Mid-band channels outperform their low-band counterparts due to higher bandwidth, while NR channels show marginal improvements over their LTE counterparts. Notably, ATT-b46, TMO-b41,

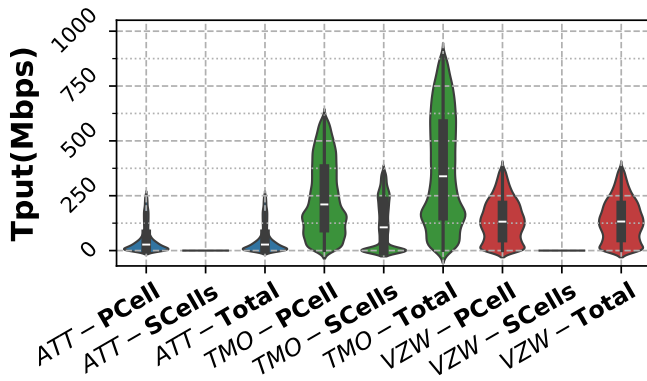
and VZW-b48 were not observed to be used for uplink transmissions. VZW-n77 demonstrates a higher median UL throughput compared to ATT-n77 and TMO-n41, suggesting that dense deployment and an increased number of beams may not necessarily translate to improved UL throughput. Fig. 10b presents the normalized UL throughput, calculated similarly to the normalized DL throughput, assuming LTE utilizes 1 stream (based on 97% of NR data using 1 stream). This assumption is made because our data lacked information on the number of uplink MIMO layers in LTE, and NR RI did not correlate with the number of NR layers in the uplink. We observe a similar trend of higher normalized UL throughput in mid-band channels compared to low-bands. The median normalized UL throughput for most representative LTE and NR channels surpasses their DL counterparts. All representative channels, except ATT-n5, TMO-n71, and TMO-b12, exhibit median normalized throughput exceeding 2 bit/s/Hz/stream. The reduced number of uplink layers likely enhances stream robustness against fading and errors.

Fig. 11a shows the comparison of UL MCS index utilized in the campaign. These values directly correlate to the normalized UL throughput, as expected given the predominant utilization of 1 layer in UL transmissions. Fig. 11b compares the usage of modulations in UL transmissions. Notably, the Pi/2-BPSK modulation, introduced in the 5G specification to improve power efficiency and reduce peak-to-average power ratio (PAPR) at a lower data rate, is utilized sparingly: most usage by TMO-n71 of 5% while other NR channels shows <1% usage. Rather, there is a notable usage of 256-QAM, particularly >40% of total usage in ATT-n77, VZW-n77, and VZW-b66, leading to a higher normalized UL throughput.

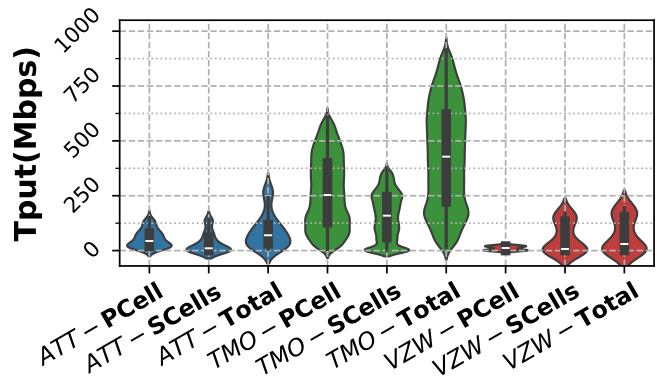
While uplink aggregation is possible between one LTE and one NR channel in the NR-NSA deployment, we only focus on comparing LTE and NR performance: there are no uplink channel aggregations observed within either LTE or NR deployments. Unlike downlink throughput, our analysis suggests that uplink throughput is not directly correlated with coverage density. Therefore, operators should focus on expanding the implementation and utilization of uplink CA to enhance uplink performance.

E. Comparison of MIMO Performance in NR and LTE

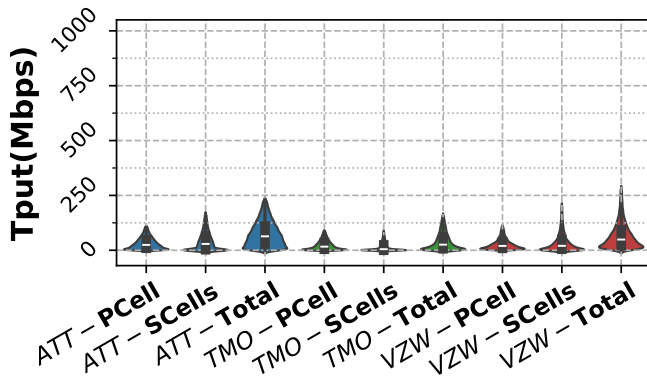
1) *Analysis of MIMO performance in terms of RI and MIMO modes:* In both LTE and NR, RI is the MIMO channel rank as calculated by the UE and transmitted back to the BS for MIMO layer decision. Since the RI metric is computed using a proprietary algorithm and not specified in the 3GPP standard, it may not reflect the actual number of spatial stream utilized in the MIMO transmission. However, we observe a strong positive correlation (Pearson coefficient of 0.95) between RI and the number of spatial streams utilized in our NR data, indicating the practicality of RI metric for this analysis. Fig. 12 shows the comparison of RI for the three operators on the representative low- and mid-band channels selected in a previous section. The data for each channel is categorized by MIMO modes (*i.e.*, 2x2, 4x4) as reported by XCAL. First, we observe that the NR low-band channels on



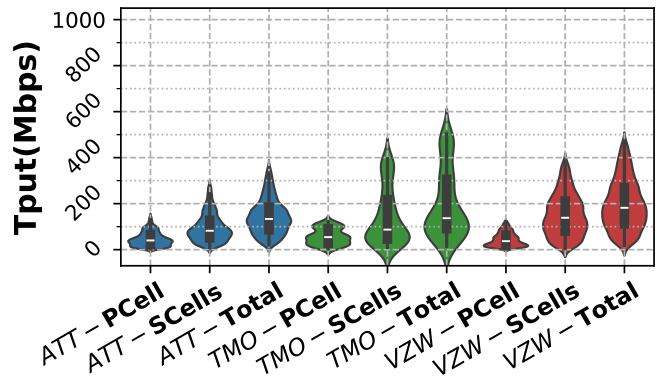
(a) NR CA throughput.



(b) NR CA throughput for CA > 1.



(c) LTE CA throughput.



(d) LTE CA tput. b46 and b48 are included.

Fig. 9: DL CA throughput performance between operators in NR and LTE

all operators do not utilize 4x4 MIMO modes, while the LTE counterparts do. Fig. 12a compares the RI value between NR and LTE channels of ATT. We observe an RI value of 2 being the most common in all channels, even when 4x4 MIMO mode is available. For instance, less than 20% of data on ATT-n77 reported an RI of 4 even when the 4x4 mode is used, while RI 4 is not seen in the corresponding b2 and b12 channels. Fig. 12b similarly shows an RI value of 2 being most common for TMO, with the exception of n41 and n71 using 2x2 mode, where the majority of the data had an RI of 1. Fig. 12c also demonstrates an RI value of 2 being most used for VZW, except for n5 with 2x2 and b13 with both 2x2 and 4x4 modes.

This result is very significant since it indicates that even though higher-order MIMO modes may be implemented, the physical channel rank may not support all available MIMO layers. This suggests that increasing MIMO order in future generations may not be the best way to improve throughput in the real-world. In fact, TMO-n41 has the best throughput performance, but it achieves this with fewer MIMO layers on average compared to ATT-n77 and VZW-n77, which are all mid-band NR channels.

2) *Analysis of MU-MIMO in NR*: While operators claim to have implemented 5G MU-MIMO in test settings [28, 29], its widespread deployment remains uncertain. To address this question, we utilize the PMI which is a part of the CSI feedback to the BS. Moreover, it conveys information about the precoding matrix that should be used in the downlink transmission. Utilizing XCAL, we collected PMI values from

all the UEs and observed PMI with indices: $i(1;1)$, $i(1;2)$, $i(1;3)$, and $i(2)$. This indicates the usage of Type 1-Single Panel codebook with 2–4 MIMO layers (refer to clause 5.2.2.2.1 in [4]). Further, we analyzed the RRC messages captured in all of our UEs and only found “mimo-Parameters > codebookParameters > typeI > singlePanel > mode := mode1” message transmitted from UEs to the base station. This indicates the capability limitation of UEs to the Type1-Single Panel codebook (refer to “CodebookParameters” subsection of clause 6.3.3 in [25]). Type 1 codebooks are used for Single User-MIMO (SU-MIMO) and only use a single beam to calculate CSI feedback [30]. Lastly, we did a stationary experiment in Minneapolis in November 2023, where we initiated downlink traffic with up to 4 UEs on the same operator, observing their exact RB allocation in the radio frame. Our hypothesis is that when MU-MIMO is enabled, at least one RB will be allocated in the same slot to two different UEs. We did not observe this in our data. While these findings do not confirm operator deployment of MU-MIMO, they strongly suggest that even if deployed, its use would be limited by current UE capabilities.

F. Comparison of Latency Performance in TMO Networks

We conducted a focused latency measurement in Minneapolis during March 2024, comparing the LTE and NR performance. Specifically, we focus on TMO, which is the only operator that has deployed NR in both SA and NSA modes. Similar to our throughput measurement campaigns, we

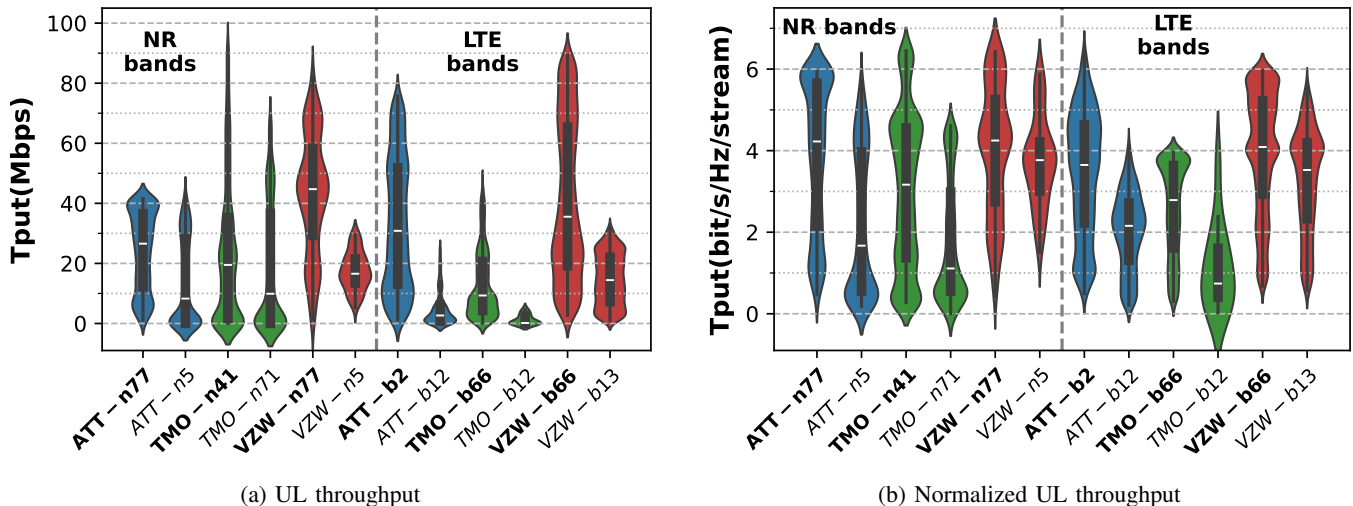


Fig. 10: UL throughput comparison of NR and LTE in low-bands (normal) and mid-bands (bolded)

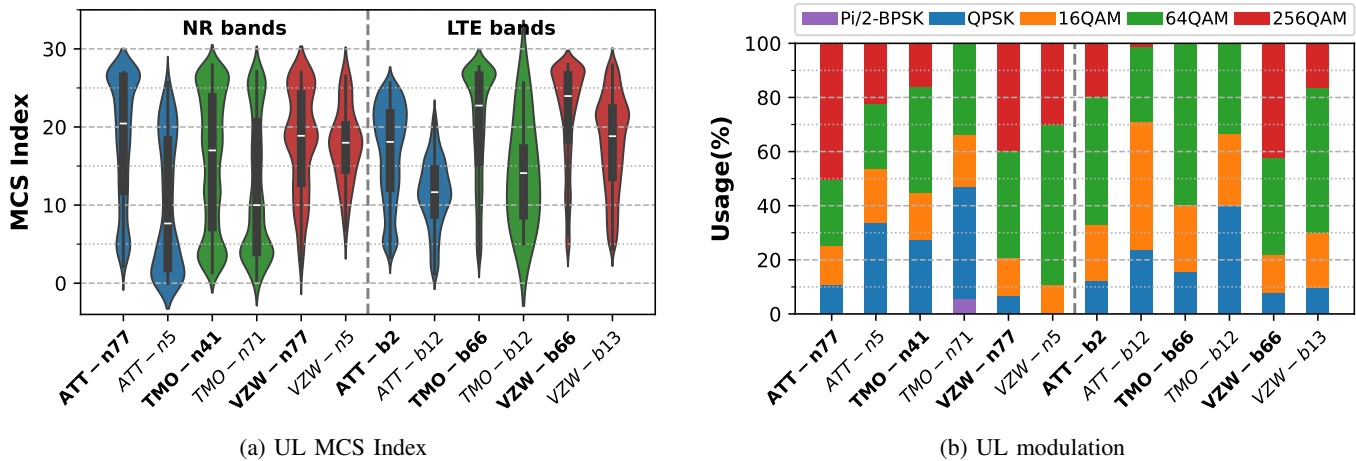


Fig. 11: Comparison of uplink MCS, CQI, TX power, and modulation of NR and LTE in low-bands (normal) and mid-bands (bolded).

collected data while driving, using $6 \times S22+$. Using XCAL, we collected signal parameters and round-trip latency results using the included ping tool. We defined two ping targets: Google’s cloud DNS server (8.8.8.8) and AWS Local Zone (server located in the same city as the end-user) [31]. Additionally, we utilized XCAL to limit the phones to the following networks and bands: SA-n71, SA-n41, NSA-n71, NSA-n41, LTE-b14 and LTE-b41. This resulted in 12 distinct data categories, each containing an average of 1,774 data points (*i.e.*, ~ 30 minutes of data collection per category).

We observe higher latency to Google DNS compared to Local Zone, which is an expected behavior. Hence, Fig. 13a shows the combined latency results (ping to Google and Local Zone) across all bands for brevity. Among the network types, SA bands exhibit the best latency performance, likely due to their simpler architecture. NSA bands, which combine NR and LTE, achieve the next best results. Fig. 13b also combines the RSRP measured for the Google and Local Zone measurements. Since both NSA-n71 and NSA-n41 utilize either b2 or b66 as the anchor LTE band, we separate those categories with “LTE” or “NR” suffixes to indicate if the RSRP is from the anchor LTE or the secondary NR channel. As expected, we observe

higher RSRP on lower-band channels. Interestingly, the LTE anchor channels in NSA bands exhibit a wider spread of RSRP values (-110 to -80 dBm). This lower and more variable RSRP in the LTE channels, combined with the overhead of using both NR and LTE, likely contributes to the slightly higher latency of NSA compared to SA bands. However, both SA and NSA offer significant latency improvements over traditional LTE.

V. CONCLUSIONS AND FUTURE WORK

We have presented a comprehensive, real-world evaluation of the performance of low- and mid-band 4G and 5G networks, examining the contribution of various system parameters—such as SSB index, RSRP, modulation, and MIMO—to throughput and latency, and presented conclusions on the reasons for the improvement in 5G throughput over 4G for all three US operators. It is clear from the data and analyses that the high downlink throughput achieved by mid-band NR channels can be attributed primarily to the higher channel bandwidth and improved signal strengths. When normalized over bandwidth and number of MIMO streams, there is only a marginal improvement in throughput over NR, except for

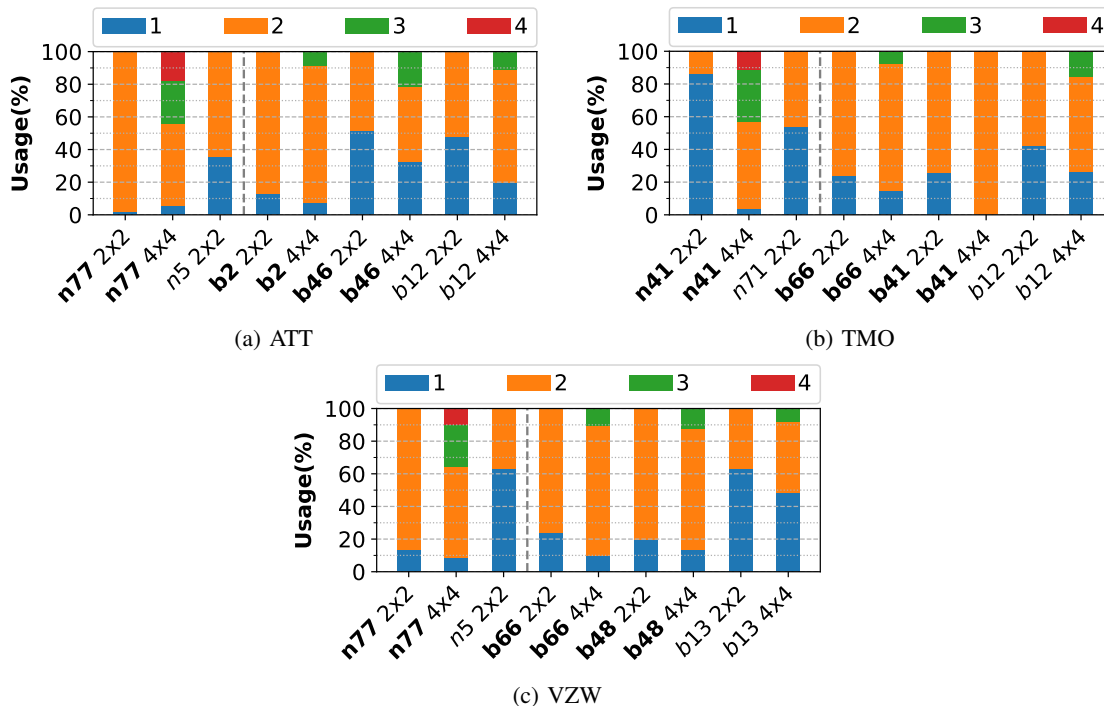


Fig. 12: RI values for the operators and MIMO modes in low-bands (normal) and mid-bands (bolded).

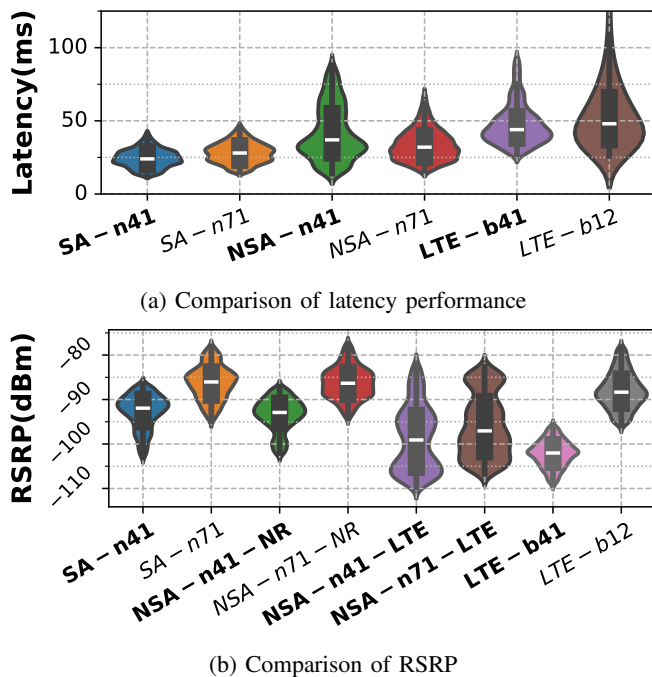


Fig. 13: Comparison of latency performance and RSRP in TMO low-bands (normal) and mid-bands (bolded)

TMO in n41 where we show that the dense deployment and larger number of beams used deliver higher signal strength on average, leading to improved spectral efficiency through the use of higher modulation modes such as 256 QAM. VZW in n77 uses fewer beams and less dense deployments thus leading to lower normalized throughput compared to other operators. On the other hand, the 5G uplink performance only shows marginal improvement over 4G due to the lower number of MIMO streams. Regarding MIMO performance, we observed

a marginal increase in the usage of the full capability 4x4 MIMO with 4 layers in NR: this indicates that increasing MIMO modes beyond 4x4 may not be the right approach to increasing throughput since the physical channel may not have sufficient diversity to support more than 4 layers. The absence of observed MU-MIMO deployment in our measurement campaign is confirmed through RRC messages and a focused experiment with multiple UEs, though it may be attributed to limitations in the capabilities of the UEs available at the time of data collection. We also compared the aggregated DL throughput performance in NR and LTE. Supporting the prior conclusion, TMO shows significantly high throughput within its NR PCell and SCells due to its dense deployment and usage of multiple beams, as well as the availability of secondary NR channels. In LTE, we observed the usage of shared CBRS (b48) and unlicensed 5 GHz (b46) bands in CA, which showed DL throughput comparable to NR CA by ATT and VZW. For uplink, we observe limited conclusion: MCS directly correlates to normalized UL throughput, rather than dense deployments and number of beams. Additionally, there is no aggregation observed in LTE channels nor in NR channels. Lastly, we observed significant 5G latency improvements over 4G on TMO, with the SA configuration delivering the best performance due to its simpler architecture and TMO's denser deployment strategy.

The cellular industry will continue to innovate and deploy new cellular technologies, with governmental agencies opening new spectrum for wireless uses. Recently, the US National Telecommunications and Information Administration (NTIA) announced the intent to study the lower 3 GHz (3.1-3.45 GHz), the 7 GHz band, and other bands for future wireless broadband uses [32]. These new spectrum bands will further increase 5G/NextG capabilities by offering increased bandwidth. On

the other hand, the rapid evolution of UE capabilities is further evidenced by a recent report showcasing stationary MU-MIMO experiments using the latest devices [33]. This highlights the potential for newer devices to support features like MU-MIMO that may not have been widely adopted or accessible during our data collection period. While operators and device manufacturers strive to implement and optimize new 5G features like MU-MIMO and higher-order modulation, their effectiveness often relies on favorable signal conditions facilitated by denser deployments and an increased number of beams. Therefore, our ongoing research will focus on continuously evaluating these 5G improvements: by quantifying the improvement of various features, such analyses are crucial in informing the development of future standards and deployment architectures. We provided public access to our data at <https://dx.doi.org/10.21227/64wp-sy79>.

REFERENCES

- [1] J. Carpenter, W. Ye, F. Qian, and Z.-L. Zhang, "Multi-modal vehicle data delivery via commercial 5G mobile networks: An initial study," in *2023 IEEE 43rd International Conference on Distributed Computing Systems Workshops (ICDCSW)*. IEEE, 2023, pp. 157–162.
- [2] T. E. Bogale and L. B. Le, "Massive MIMO and mmWave for 5G wireless HetNet: Potential benefits and challenges," *IEEE Vehicular Technology Magazine*, vol. 11, no. 1, pp. 64–75, 2016.
- [3] A. N. Uwaechia and N. M. Mahyuddin, "A comprehensive survey on millimeter wave communications for Fifth-Generation Wireless Networks: Feasibility and challenges," *IEEE Access*, vol. 8, pp. 62 367–62 414, 2020.
- [4] 3rd Generation Partnership Project, "TS 38.214 5G; NR; Physical layer procedures for data version 17.1.0 Release 17," 2022.
- [5] Nokia, "5G spectrum bands explained," <https://www.nokia.com/thought-leadership/articles/spectrum-bands-5g-world/>, accessed: 2023-11-26.
- [6] M. Dano, "The quiet brilliance of T-Mobile's 5G spectrum strategy," 2022, accessed: 2023-11-26. [Online]. Available: <https://www.lightreading.com/5g/the-quiet-brilliance-of-t-mobile-s-5g-spectrum-strategy>
- [7] M. Allevan, "AT&T takes advantage of early C-band clearing," 2023, accessed: 2023-11-26. [Online]. Available: <https://www.fiercewireless.com/5g/att-takes-advantage-early-c-band-clearing>
- [8] K. Schulz, "Verizon turbo charges its 5G network with the addition of more spectrum," 2023, accessed: 2023-11-26. [Online]. Available: <https://www.verizon.com/about/news/verizon-5g-network-addition-more-spectrum>
- [9] Y.-N. R. Li, B. Gao, X. Zhang, and K. Huang, "Beam management in millimeter-wave communications for 5G and beyond," *IEEE Access*, vol. 8, pp. 13 282–13 293, 2020.
- [10] A. Narayanan, M. I. Rochman, A. Hassan, B. S. Firman-syah, V. Sathya, M. Ghosh, F. Qian, and Z.-L. Zhang, "A comparative measurement study of commercial 5G mmWave deployments," in *IEEE INFOCOM 2022-IEEE Conference on Computer Communications*, 2022, pp. 800–809.
- [11] 3rd Generation Partnership Project, "TS 38.213 5G; NR; physical layer procedures for control 17.1.0 Release 17," 2022.
- [12] O. Elijah, C. Y. Leow, T. A. Rahman, S. Nunoo, and S. Z. Iliya, "A comprehensive survey of pilot contamination in massive MIMO—5G system," *IEEE Communications Surveys & Tutorials*, vol. 18, no. 2, pp. 905–923, 2015.
- [13] J. Jose, A. Ashikhmin, T. L. Marzetta, and S. Vishwanath, "Pilot contamination and precoding in multi-cell TDD systems," *IEEE Transactions on Wireless Communications*, vol. 10, no. 8, pp. 2640–2651, 2011.
- [14] D. López-Pérez, A. De Domenico, N. Piovesan, G. Xinli, H. Bao, S. Qitao, and M. Debbah, "A survey on 5G radio access network energy efficiency: Massive MIMO, lean carrier design, sleep modes, and machine learning," *IEEE Communications Surveys & Tutorials*, vol. 24, no. 1, pp. 653–697, 2022.
- [15] 3rd Generation Partnership Project, "TS 38.101-1 5G; NR; user equipment (UE) radio transmission and reception; Part 1: Range 1 standalone 17.5.0 Release 17," 2022.
- [16] M. I. Rochman, V. Sathya, D. Fernandez, N. Nunez, A. S. Ibrahim, W. Payne, and M. Ghosh, "A comprehensive analysis of the coverage and performance of 4G and 5G deployments," *Computer Networks*, vol. 237, p. 110060, 2023.
- [17] B. Fletcher, "CBRS boosts Verizon 4g speeds 79% but power levels show limits," <https://www.fiercewireless.com/tech/cbrs-boosts-verizon-4g-speeds-79-power-levels-show-limits>, accessed: 2023-11-26.
- [18] V. Sathya, M. I. Rochman, and M. Ghosh, "Measurement-based coexistence studies of LAA & Wi-Fi deployments in Chicago," *IEEE Wireless Communications*, vol. 28, no. 1, pp. 136–143, 2020.
- [19] Accuver. XCAL - PC based advanced 5G network optimization solution. [Online]. Available: <https://www.accuver.com/sub/products/view.php?idx=6>
- [20] 3rd Generation Partnership Project, "TS 38.104 5G; NR; base station (BS) radio transmission and reception 17.5.0 Release 17," 2022.
- [21] —, "TS 38.211 5G; NR; physical channels and modulation 17.1.0 Release 17," 2022.
- [22] —, "TS 38.215 5G; NR; physical layer measurements 17.1.0 Release 17," 2022.
- [23] —, "TS 38.300 5G; NR; NR and NG-RAN overall description; stage-2 17.0.0 Release 17," 2022.
- [24] —, "TS 38.306 5G; NR; user equipment (UE) radio access capabilities 17.0.0 Release 17," 2022.
- [25] —, "TS 38.331 5G; NR; radio resource control (RRC); protocol specification 17.1.0 Release 17," 2022.
- [26] iperf3 - the TCP, UDP and SCTP network bandwidth measurement tool. [Online]. Available: <https://iperf.fr/>
- [27] Samsung, "Dynamic Spectrum Sharing," <https://images.samsung.com/is/content/samsung/assets/>

- global/business/networks/insights/white-papers/0122_dynamic-spectrum-sharing/Dynamic-Spectrum-Sharing-Technical-White-Paper-Public.pdf, 2021, accessed: 2024-12-30.
- [28] M. Allevin, "T-Mobile's 5G network gets capacity boost from MU-MIMO: report," <https://www.fiercewireless.com/tech/t-mobiles-5g-network-gets-capacity-boost-mu-mimo-report>, accessed: 2024-05-09.
- [29] Signals Research Group, "5G: The greatest show on earth! vol. 33: MU-MIMO and the tower of power," <https://signalsresearch.com/issue/5g-the-greatest-show-on-earth-33/>, accessed: 2024-05-09.
- [30] Z. Qin and H. Yin, "A review of codebooks for CSI feedback in 5G New Radio and beyond," *arXiv preprint arXiv:2302.09222*, 2023.
- [31] AWS, "AWS local zones," <https://aws.amazon.com/about-aws/global-infrastructure/localzones/>, 2020, accessed: 2024-05-13.
- [32] National Telecommunications and Information Administration. (2023) The national spectrum strategy. [Online]. Available: https://www.ntia.gov/sites/default/files/publications/national_spectrum_strategy_final.pdf
- [33] Signal Research Group, "5G Multi-User MIMO - it isn't just for downlink anymore," <https://signalsresearch.com/issue/5g-multi-user-mimo-it-isnt-just-for-downlink-anymore/>, 2024, accessed: 2024-12-30.